

Assessing the GOES-16 ABI solar channels calibration using deep convective clouds

Hyelim Yoo^a, Fangfang Yu^a, Xiangqian Wu^b, Haifeng Qian^a, Robert Iacovazzi^a

^a ERT, Inc. Laurel, MD 20707 USA

^b NOAA, NESDIS, STAR, College Park, MD 20740 USA

ABSTRACT

Tropical deep convective clouds (DCCs) are thick, bright, cold, and their reflectance is considered stable. Thus, DCCs can be used to calibrate visible/near infrared (VNIR) channels of satellite instruments. Previous studies report how DCCs are identified by providing specific brightness temperature thresholds and are used for calibration purpose as an invariant target for solar channels. On 19 November 2016, the Geostationary Operational Environment Satellite-R Series (GOES-R) was successfully launched and became GOES-16 after it reached the geostationary orbit on 29 November 2016. The Advanced Baseline Imager (ABI) instrument on-board GOES-16 has 16 multi-spectral bands (0.47 - 13.3 μ m) which have more accurate and frequent radiometric calibration information than previous GOES satellite series. Assessment and monitoring of the GOES-16 ABI VNIR channels calibration using DCC method is a main objective of this study. The target region is a 20°N-20°S and 119.5°W-59.5°W centered on the GOES-16 ABI check-out spatial domain (at 0.0°N, 89.5°W). This work is expected to provide useful information regarding the ABI radiometric calibration stability and such calibration stability of the ABI VNIR channels will be compared the results with other methods (e.g., ray-matching and desert) in the near future.

Keywords: GOES-16, ABI, calibration, DCC

1. Introduction

Deep Convective Clouds (DCCs) can be assumed nearly a Lambertian reflectance and they can provide an invariant monthly mean albedo. They are common in the tropical regions and located at the tropopause where water vapor absorption effect on radiative transfer is minimal. So, DCCs can be considered as an ideal constant Earth target for radiometric calibration of satellite imaging instrument VNIR channels. The Advanced Baseline Imager (ABI) is the primary instrument of the GOES-16 satellite for Earth's weather and ocean monitoring. Unlike previous and current GOES series, the ABI has six spectral bands covering VNIR wavelengths that provide much better temporal and spatial resolution. The ABI has great improvements in terms of radiometric calibration and noise compared to its similar instrument Advanced Himawari Imager (AHI) onboard Himawari-8 satellite (Efremova et al. 2016). The DCC method can be expected to provide an opportunity to develop, test and examine the calibration/validation tool for the ABI. Also, this study supports the ABI Level 1b Post-Launch Product Test.

In this paper, we focus on the assessment and monitoring of the GOES-16 ABI VNIR channels over the identified DCC pixels. The Visible Infrared Imaging Radiometer Suite (VIIRS) onboard Suomi-National Polar-orbiting Partnership (SNPP) spacecraft DCC results are compared with the ABI results in terms of time-series and frequencies of the DCC reflectance for the VNIR channels.

2. Methodology and data

Data collected from the ABI full disk Level 1b data at the six VNIR channels and VIIRS Sensor Data Record (SDR) data during January 18 – June 4, 2017 is used in this study. The spatial resolution of the ABI VNIR channels have a relatively coarse compared to the VIIRS: VIIRS M (I) band has 750 m (375 m) resolution whereas the ABI Bands 1, 3, and 5 have a 1 km resolution, the Band 2 has a 0.5 km resolution, the Bands 4 and 6 have a 2 km resolution, respectively. To identify DCC pixels, we follow the baseline DCC technique by Doelling et al. (2013). Any pixels of GOES-16 Level 1b falling between 20°N-20°S and 119.5°W-59.5°W are considered, and for a given pixel a spatial uniformity threshold is applied by calculating the standard deviation of the center pixel and its surrounding eight pixels. Statistics for the DCC pixels between 17:00-18:59 UTC time are derived at 2 km resolution for the ABI and 750 m for the VIIRS using the following thresholds: Standard deviation threshold less than 3 % at 0.64 μ m and less than 1 K at 11 μ m; Brightness temperature threshold less than 205 K at 11 μ m; Solar/viewing zenith angles less than 40° to take advantage of the Lambertian part of the DCC reflective area. Also, sun-glint area is excluded and data quality flag is considered to identify DCC pixels. The sun-glint angle calculation is based upon the equation of Yu and Wu (2016)

$$\cos(\eta) = \cos(\theta_s)\cos(\theta_v) + \sin(\theta_s)\sin(\theta_v)\cos(180 - \varphi)$$

where η is the sun-glint angle, θ_s and θ_v are the solar zenith angle and satellite viewing zenith angle, respectively, and φ is the relative azimuth angle between solar and viewing azimuths.

To compare the ABI DCC identification by GOES-16 with those from the VIIRS data, the Spectral Band Adjustment Factor (SBAF) should be included in the analysis to correct radiometric biases arising due to the slight Spectral Response Function (SRF) differences between the two instruments (Figure 1). The SRF at the ABI Band 1 (0.47 μ m) is broader than that of VIIRS M3 Band and the SRFs at the other ABI bands are very similar with the VIIRS I/M bands.

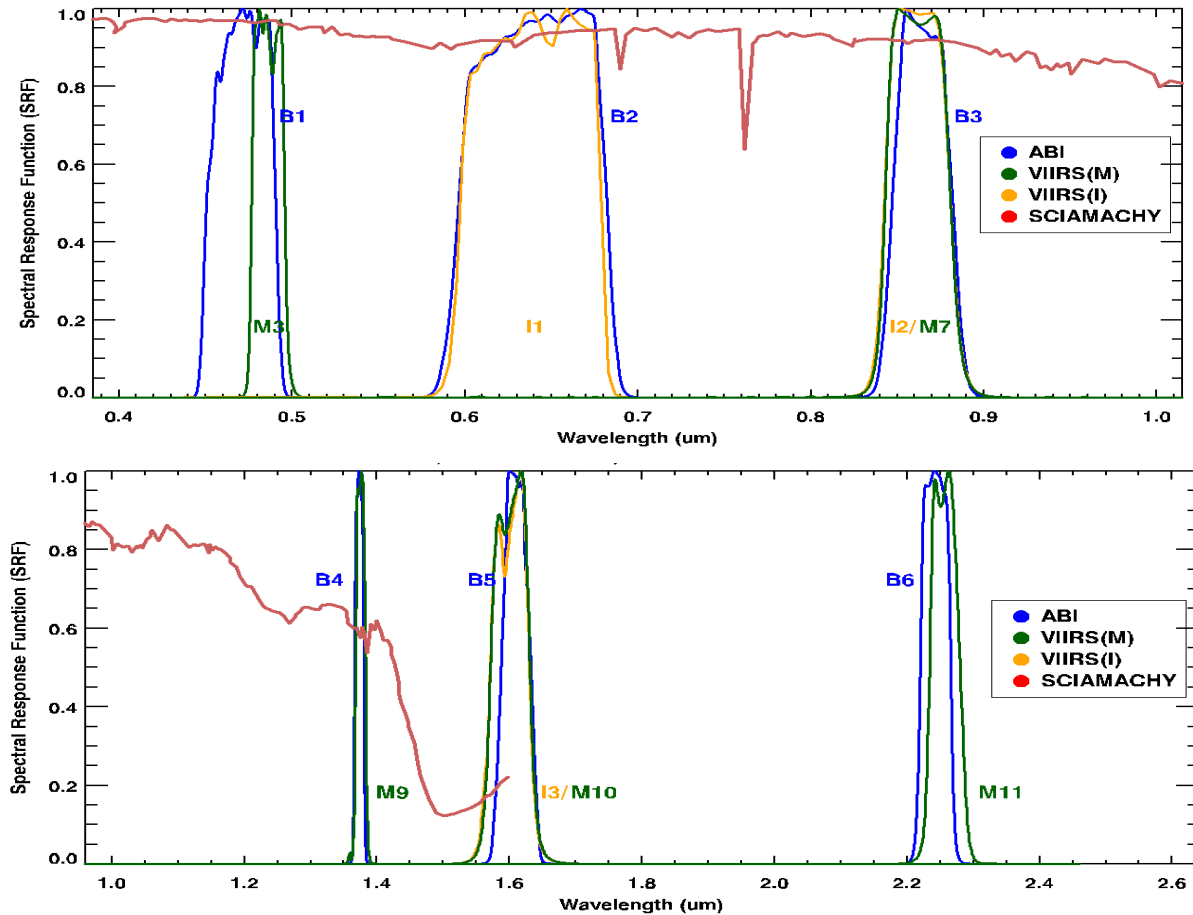


Figure 1. A comparison among the ABI SRFs, the VIIRS SRFs, and the SCIAMACHY SRFs.

In this study, the SBAFs derived from the SCanning Imaging Absorption spectrometer for Atmospheric CHartographY (SCIAMACHY) is provided by NASA Langley center. The linear fit SBAF with SNPP-VIIRS Non-Government (NG) SRF over the precise DCC earth spectra is generated from the SBAF web-tools because NOAA uses the VIIRS NG SRFs version for the operational calibration. Table 1 summarizes the SBAF slope and offset for the ABI VNIR channels. Note that there is no SBAF for the ABI Band 6 ($2.2\text{ }\mu\text{m}$) so we assume that the slope is 1.0 and the offset is 0.0 because of the similarity of the SRFs between the ABI Band 6 and the VIIRS M11 Band. The corrected reflectance with the SBAF coefficients is calculated as follows (Yu and Wu, 2016):

$$\text{reflectance}_{\text{VIIRS,ABI}} = (\text{reflectance}_{\text{ABI}} - \text{SBAF_offset}) / \text{SBAF_slope}$$

where $\text{reflectance}_{\text{VIIRS,ABI}}$ is the corrected reflectance corresponding to the ABI reflectance based on the SBAFs. In addition, reflectance of the identified DCC pixels from both the ABI and VIIRS is corrected with Hu et al. (2004) model for Angular Distribution Model (ADM) adjustment.

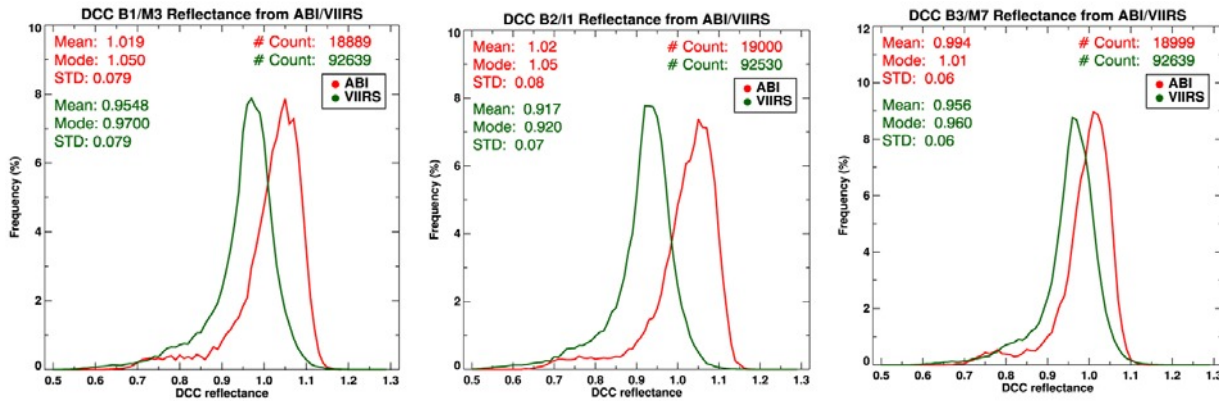
Table 1. The SBAF (ABI/VIIRS) slope and offset at the six VNIR channels.

SBAF	ABI	B1	B2	B3	B4	B5	B6
VIIRS		M3	I1	M7	M9	M10	M11
DCC	Slope	0.991	1.000	0.998	0.996	1.031	1.0
	Offset	0.01029	-0.000288	0.001004	0.00605	0.002848	0.0

3. Results

3.1. A comparison of frequencies of the DCCs reflectance

Figure 2 displays a comparison of frequencies of the DCCs reflectance from both the ABI and VIIRS data during Jan. 18 - Jan. 22, 2017. After the GOES-16 satellite is launched, Level 1b data started to be provided through NOAA Environmental Satellite Product and Distribution System (ESPDS) Product Distribution and Access (PDA). The ABI results are comparable for capturing the general image features seen from the VIIRS retrievals, except for slight differences in its magnitude. Overall, the ABI results produce somewhat brighter reflectance for all six VNIR channels, especially ABI Bands 1-3 which have wavelengths less than $1\text{ }\mu\text{m}$. Mode and mean statistics of the DCC pixels are computed for the bands less than $1\text{ }\mu\text{m}$ and median and mean values are provided for the bands greater than $1\text{ }\mu\text{m}$ (Bhatt et al. 2014). As mentioned earlier, the identified DCC pixels from the ABI (VIIRS) are retrieved at 2 km (750 m) resolution in this study. The GOES-16 is a geostationary satellite, thus the ABI DCC pixels should be more collected during specific time range although the retrieval resolution is coarser than the VIIRS sensor onboard a sun-synchronous orbit. However, the DCC pixels identified from the ABI during this period have a lot data quality flag as 2, which means out of range pixel saturation. This is especially true for Bands 1-3, and may explain why the number of VIIRS DCC pixels is much more than the number of ABI DCC pixels in the initial time period.



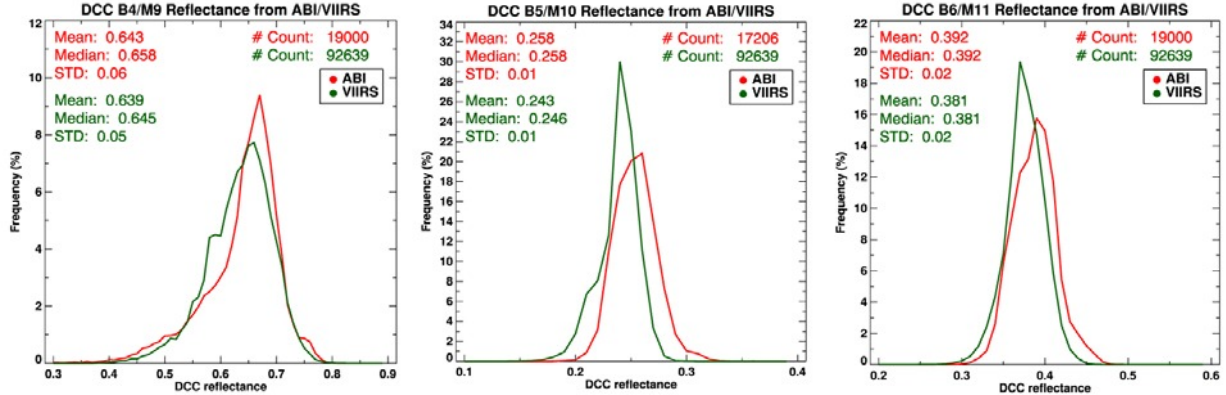


Figure 2. A comparison of histograms of the identified DCCs reflectance from both the ABI and VIIRS during January 18 - 22, 2017. The y-axis is the DCC frequency (%) and the x-axis is the identified DCC reflectance.

The ABI sensor has experienced some changes in solar calibration coefficients after its launch, thus the comparison of the DCC results depends on which time period is used due to the solar calibration instability. We selected May 8-15 period which did not show any change in solar calibration offset. Unlike the initial time period of the ABI DCC results, the ABI DCC reflectance during May 8-15 somewhat increased from 0.3 % to 2 % except for ABI Band 5 and the number of the identified DCC pixels significantly increased as well in the all VNIR channels. These features are particularly remarkable for the ABI Bands 1-3 (Fig. 3). It seems that there are some changes in implementations of solar calibration coefficient update and in improvements on image navigation and registration for ABI. For the reasons why the number of ABI DCC pixels increase, the ground processing system updated the threshold of out of saturation range in March. As a result, the number of ABI DCC pixels is much more identified during May 8-15, 2017 due to a remarkable decrease in the screened out pixels whereas the VIIRS DCC pixels remain similar. Note that the VIIRS DCC reflectance seems to be stable in the all VNIR channels.

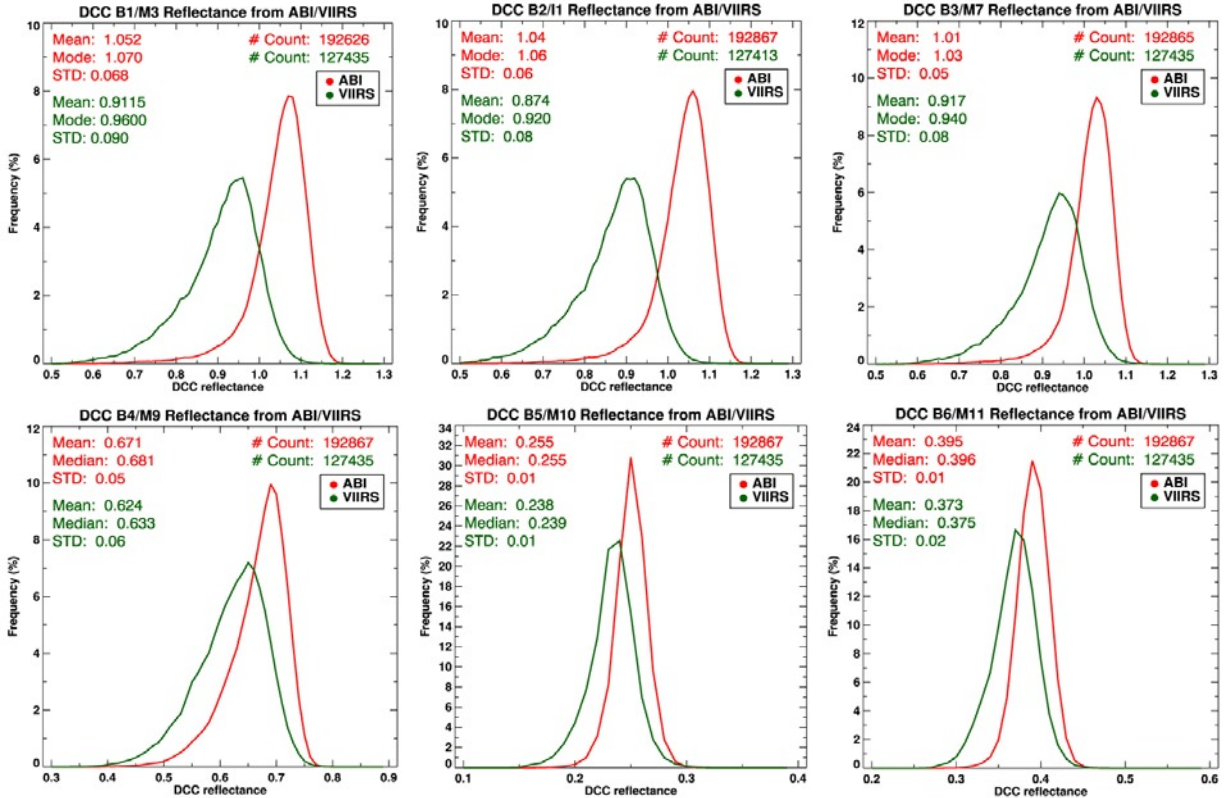


Figure 3. Same as Figure 2 except for May 8-15, 2017.

Figure 4 compares the spatial distributions of the identified DCCs from both the ABI and VIIRS during Jan. 18-22 and May 8-15. The red dot symbol indicates for the ABI DCCs and the green dot symbol is for the VIIRS DCCs. Most DCCs developed interior continental region over the South America during Northern Hemisphere (NH) winter time, whereas they moved toward high latitudes and more over oceans during NH summer time. The annual cycles of DCCs are different over land and ocean due to differences in cloud particle size/type, aerosol amount/type, and convection source (Wang and Cao, 2014) and these can affect DCCs reflectance patterns and magnitudes.

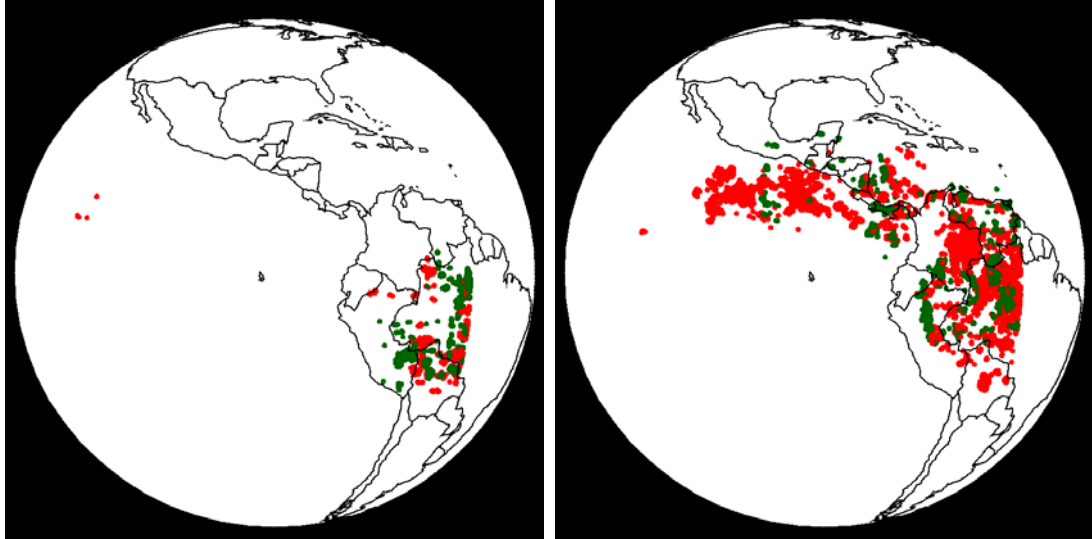


Figure 4. Geographic distributions of the identified DCC pixels from both the ABI and VIIRS during Jan. 18-22, 2017 (left panel) and May 8-15, 2017 (right panel).

3.2. Time series of DCCs reflectance

Time series of the daily mean DCCs reflectance from the ABI (left panel) and the VIIRS (right panel) during Jan. 18 – Jun. 4, 2017 for the all six VNIR channels is shown in Figure 5. It can be seen that the ABI results show large variations in the DCCs reflectance monitoring than the VIIRS. Two plausible causes are considered. Firstly, the solar calibration coefficients are unstable for the ABI, which is captured in time series of the VNIR channel gain values (not shown). For example, a few (nearly 10 %) jumps in the solar calibration derived from instrument gain are seen during this period, which have been identified to be caused by ground processing software errors that lead to the Level 1b data generation anomalies presented here. This issue is still being resolved by the GOES-R Ground Segment Project. Another possible cause is associated with differences between the ABI and VIIRS either a specific threshold value of saturation range for the DCC pixels or data quality flag criterion.

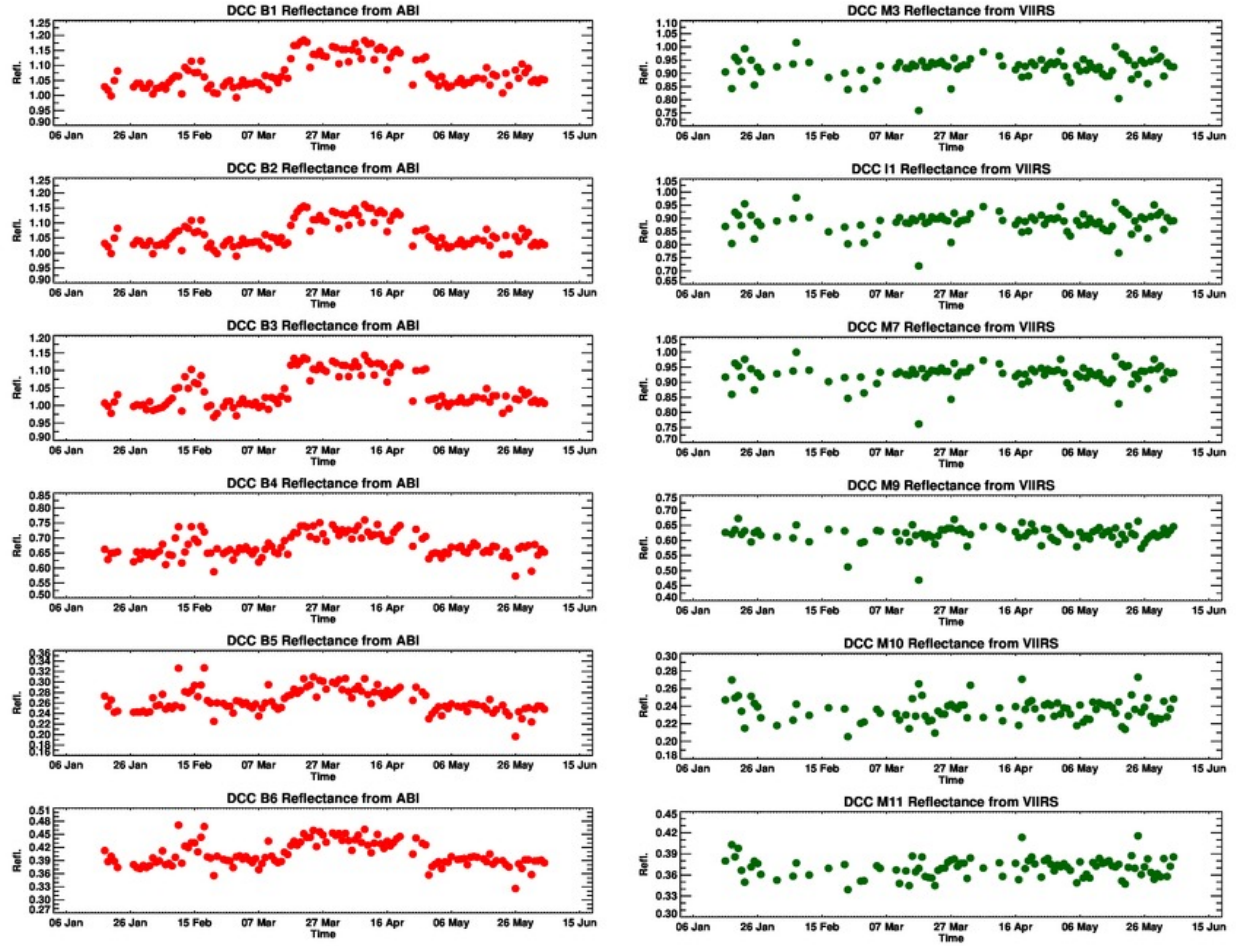


Figure 5. Time series of the DCCs reflectance from both the ABI (left panel) and the VIIRS (right panel) during Jan. 18 – Jun. 4, 2017.

4. Summary and discussion

It is important to validate radiance accuracy of the ABI's six VNIR channels. Monitoring of DCCs reflectance trending makes it possible to assess radiometric calibration stability by providing useful information. In this study, the DCCs reflectance monitoring method is used to evaluate the ABI VNIR channels radiometric calibration accuracy and stability using a reference of the VIIRS DCC retrievals. The VIIRS data has been used in validating different cloud variables and solar channel calibration stability in previous studies (Uprety et al., 2013 and Wang and Cao, 2014).

In the initial time period after the ABI launch, frequencies of the DCCs reflectance from both the ABI and the VIIRS are in a good agreement in terms of pattern and shape in spite of the existence of difference in magnitude. Also, spatial distributions of the identified DCCs from both the results are comparable. However, whereas the VIIRS DCCs reflectance trending is stable, the ABI DCCs reflectance showed more variations of their magnitudes. The causes of the discrepancies come from both known and unknown sources of instability in solar calibration coefficients. Further studies are needed to resolve the unknown sources of solar calibration coefficients instability and to elucidate the characteristics and identification of DCCs.

5. Acknowledgements

The authors thank to Drs. Vladimir Kondratovich, Li Zhu, and Xi Shao who work at Calibration Working Group/NOAA, flight groups, and the ABI instrument vendor. We are also grateful to NOAA anonymous reviewers for helpful comments and discussions to the manuscript. This work is funded by GOES-R program. The manuscript contents are solely the opinions of the authors and do not constitute a statement of policy, decision, or position on behalf of NOAA or the U.S. government.

6. References

- [1] Bhatt, R.; Doelling, D.R.; Wu, A.; Xiong, X.; Scarino, B.R.; Haney, C.O.; Gopalan, A., “Initial stability assessment of S-NPP VIIRS reflective solar band calibration using invariant desert and deep convective cloud targets” *Remote Sens.* 6, 2809–2826, (2014).
- [2] Doelling, D.; Morstad, D.; Scarino, B.; Bhatt, R.; Gopalan, A., “The characterization of deep convective clouds as an invariant calibration target and as a visible calibration technique” *IEEE Trans. Geosci. Remote Sens.* 51, 1147–1159, (2013).
- [3] Efremova, B.; Pearlman, A.; Padula, F.; Wu, X., “Detector level ABI spectral response function: FM4 analysis and comparison for different ABI modules” *Proc. SPIE* 9972, 99720S 10 pp, (2016).
- [4] Hu, Y.; Wielicki, B.; Yang, P.; Stackhouse, P.; Lin, B.; Young, D., “Application of deep convective cloud albedo observation to satellite-based study of terrestrial atmosphere: Monitoring the stability of spaceborn measurement and assessing absorption anomaly” *IEEE Trans. Geosci. Remote Sens.* 42, 2594–2599, (2004).
- [5] Upadhyay, S.; Cao, C.; Xiong, X.; Blonski, S.; Wu, A.; Shao, X., “Radiometric inter-comparison between Suomi NPP VIIRS and Aqua MODIS reflective solar bands using simultaneous nadir overpass in the low latitudes” *J. Atmos. Ocean. Technol.* 30, 2720–2736, (2013).
- [6] Wang, W.; Cao, C., “Assessing the VIIRS RSB calibration stability using deep convective clouds” *Proc. SPIE* 9264, (2014).
- [7] Yu, F.; Wu, X., “Radiometric Inter-Calibration between Himawari-8 AHI and S-NPP VIIRS for the Solar Reflective Bands” *Remote Sens.* 8, 165, (2016).